www.MaterialsViews.com

ADVANCED
HEALTHCARE
MATERIALS
www.advhealthmat.de

FULL PAPER

Pd-Porphyrin-Cross-Linked Implantable Hydrogels with Oxygen-Responsive Phosphorescence

Haoyuan Huang, Wentao Song, Guanying Chen, Justin M. Reynard, Tymish Y. Ohulchanskyy, Paras N. Prasad, Frank V. Bright, and Jonathan F. Lovell*

Development of long-term implantable luminescent biosensors for subcutaneous oxygen has proved challenging due to difficulties in immobilizing a biocompatible matrix that prevents sensor aggregation yet maintains sufficient concentration for transdermal optical detection. Here, Pd-porphyrins can be used as PEG cross-linkers to generate a polyamide hydrogel with extreme porphyrin density ($\approx 5 \times 10^{-3}$ M). Dye aggregation is avoided due to the spatially constraining 3D mesh formed by the porphyrins themselves. The hydrogel exhibits oxygen-responsive phosphorescence and can be stably implanted subcutaneously in mice for weeks without degradation, bleaching, or host rejection. To further facilitate oxygen detection using steady-state techniques, an oxygen-non-responsive companion hydrogel is developed by blending copper and free base porphyrins to yield intensity-matched luminescence for ratiometric detection.

1. Introduction

Oxygen plays a vital role in physiological processes and abnormal levels are linked with a multitude of pathologies such as cerebral,[1] cardiovascular,[2] and neoplastic[3] diseases. Appropriate subcutaneous tissue oxygenation is essential for wound healing.[4] To date, few minimally invasive methods have been described for monitoring of oxygen directly in subcutaneous tissue that are suitable for long-term monitoring. A variety of methods have emerged to gauge the concentration of oxygen in tissues in vivo, such as direct transdermal insertion of electrodes and probes, and examination of optical and magnetic properties of blood.[5] Non-invasive methods based on oxy- and deoxy-hemoglobin optical and magnetic properties are widely used, but only examine blood oxygenation within vessels, which is not a necessarily reliable indicator of tissue oxygenation. Perhaps the most direct methods to measure tissue oxygenation are electrochemical and phosphorescence quenching methods, both of which involve the use of exogenous probes or sensors.[5] Electrochemical methods are effective for in vivo measurements, but necessitate the use of probes that pass from inside the body to outside, making long-term monitoring challenging.[6] Phosphorescence quenching based on triplet state relaxation by molecular oxygen have proven useful for oxygen sensing. Porphyrins are known as excellent theranostic agents[7] and Ru(II)-,[8] Pd(II)-,[9] and Pt(II)-.[10,11] 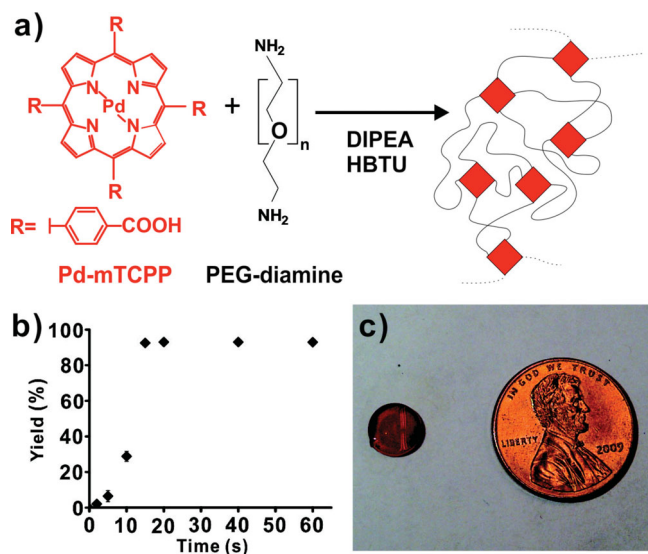porphyrins, have been validated as oxygen responsive probes. These molecules have near infrared (NIR) emission, high stability, long-life times, and good biocompatibility.[12–15] Pd- and Pt-porphyrin derivatives have emerged as an accurate method to measure oxygenation in cell cultures[16–18] and in vivo,[19–22] being well-suited to examine levels of hypoxia within tumors.[23–25] Recent advances have used nanoparticles and microparticles for in vivo oxygen sensing applications.[26] Despite their successful use for some in vivo applications, longer-term phosphorescence quenching methods generally are limited by: 1) lack of techniques for biocompatible immobilization of the porphyrin sensor within the target tissue and 2) difficulties in obtaining an immobilized porphyrin in sufficient concentration to permit transdermal phosphorescence detection. Hydrogels are hydrophilic, water-swollen polymers ideal for implantation and have numerous diverse applications in fields such as tissue engineering, drug delivery, and have been explored as doped sensors for sensing applications.[27–34] Luminescence quenching has also been explored in other potentially implantable materials such as silicone, but such approaches face the same challenges for in vivo implantation and transdermal detection.[35] We recently demonstrated that polyethylene glycol (PEG) diamines could be condensed with free base non-metallo tetracarboxy porphyrins, resulting in a bright and biocompatible polyamide polymer resistant to degradation following weeks of implantation in vivo.[36] Based on this work, we set out to examine Pd-porphyrins as active cross-linkers to generate an oxygen-responsive hydrogel for use as an implantable, oxygen-responsive phosphorescent biomaterial.

H. Huang, W. Song, Prof. J. F. Lovell
Departments of Biomedical Engineering
and Chemical and Biological Engineering
210 Bonner Hall
University at Buffalo, Buffalo, NY 14260, USA
E-mail: jflovell@buffalo.edu
Dr. G. Chen, Dr. T. Y. Ohulchanskyy, Prof. P. N. Prasad
Institute for Lasers
Photonics and Biophotonics
428 NSC, University at Buffalo, Buffalo, NY 14260, USA
Dr. G. Chen, J. M. Reynard, Dr. T. Y. Ohulchanskyy, Prof. F. V. Bright
Department of Chemistry
511 NSC, University at Buffalo, Buffalo, NY 14260, USA

**ADVANCED
HEALTHCARE
MATERIALS**

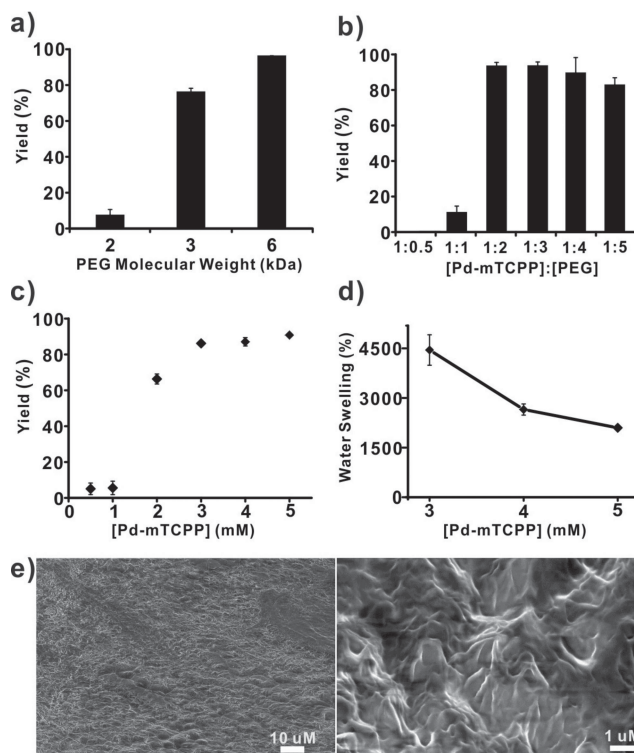www.advhealthmat.de

Materials Views

www.MaterialsViews.com

Figure 1. Pd-porphyrins as effective PEG crosslinkers to generate a hydrogel with extreme ($\approx 5 \times 10^{-3}$ M), spatially segregated porphyrin density. a) Chemical structures of Pd-mTCPP and PEG-diamines and the schematic polymer network formed following condensation. b) Rapid and complete polymerization of the PEG and porphyrin following addition of DIPEA to initiate the reaction. Mean ± std. dev. shown for $n = 3$. c) Photograph of an 8 mm hydrogel.

Figure 2. Characterization of Pd-porphyrin hydrogel formation. In otherwise equivalent conditions, polymer yield was affected by a) PEG diamine size; b) Ratio of Pd-mTCPP to PEG-diamine (6 K); and c) Pd-mTCPP concentration (with constant ratios of PEG:porphyrin:HBTU). d) Water swelling as a function of Pd-mTCPP concentration during polymerization. Mean ± std. dev. shown for $n = 3$. e) SEM of a freeze-dried portion of Pd-mTCPP hydrogel.

2. Results and Discussion

2.1. Pd-mTCPP Hydrogel Synthesis and Characterization

Based on the oxygen-sensitive phosphorescence of Pd-porphyrins, Pd-meso-tetra(4-carboxyphenyl) porphine (Pd-mTCPP) was used a cross-linker for PEG diamines (**Figure 1**a). The resulting polymer was predicted to have a highly interconnected mesh form, resulting in the spatial segregation of the porphyrins (Figure 1a). The polymerization was carried out in dimethylformamide (DMF) using O-benzotriazol-1-yl-tetramethyluronium hexafluorophosphate (HBTU) as a coupling agent and the reaction was initiated with diisopropylethylamine (DIPEA) as a base. Pd-mTCPP, PEG-diamines, and HBTU were added in a 1:2:4 ratio to achieve stoichiometric ratios of acid, base, and coupling agent groups. Addition of 0.5% DIPEA was sufficient to initiate a rapid polymerization (Figure S1, Supporting Information). The reaction completed within 20 s, resulting in the covalent incorporation of >95% of the free Pd-mTCPP into the polymer network (Figure 1b). Next, the hydrogel was generated by incubating the polymer in water to remove all DMF from the gel. The 8 mm diameter hydrogel had a smooth and reflective surface and was deeply red as a result of the extreme concentration of 5×10^{-3} M Pd-mTCPP that actively formed the unique mesh network of the hydrogel (Figure 1c).

Next, the properties of Pd-mTCPP hydrogel formation were examined. As shown in **Figure 2**a, as the molecular weight of the PEG diamines decreased from 6 K to 2 K, the polymerization

efficiency declined from over 95% to less than 10%. This demonstrates that the unique 3D mesh framework of the Pd-mTCPP hydrogels required appropriate spacing distances between alternating PEG and porphyrin units to polymerize effectively. It is noteworthy that in these experiments, lack of incorporation of Pd-mTCPP into the insoluble hydrogel does not imply that polymerization was not occurring, but rather the conditions were not appropriate for achieving a single, massively interconnected and insoluble polymer. Since PEGs carrying 2 amine groups and porphyrins carrying 4 carboxyphenyl groups were the main connective elements to the polymer, the ratio between these molecules was critical. As expected, a molar ratio of 1:2 (Pd-mTCPP:PEG-diamine) provided the highest full polymerization efficiency, since this corresponds to the stoichiometric ratio of the functional groups (Figure 2b). The concentration of Pd-mTCPP also played a vital role in the reaction. As shown in Figure 2c, with the ratio between Pd-mTCPP:PEG-diamine:HBTU fixed at 1:2:4, hydrogel generation efficiency declined dramatically as the Pd-mTCPP concentration decreased to below 2×10^{-3} M in the reaction solution. Again, this points to the requirement of a well-defined spatial arrangement between PEG and porphyrin units in the 3D polymer mesh. Among the concentrations that permitted effective

www.MaterialsViews.com

ADVANCED
HEALTHCARE
MATERIALS
www.advhealthmat.de

FULL PAPER
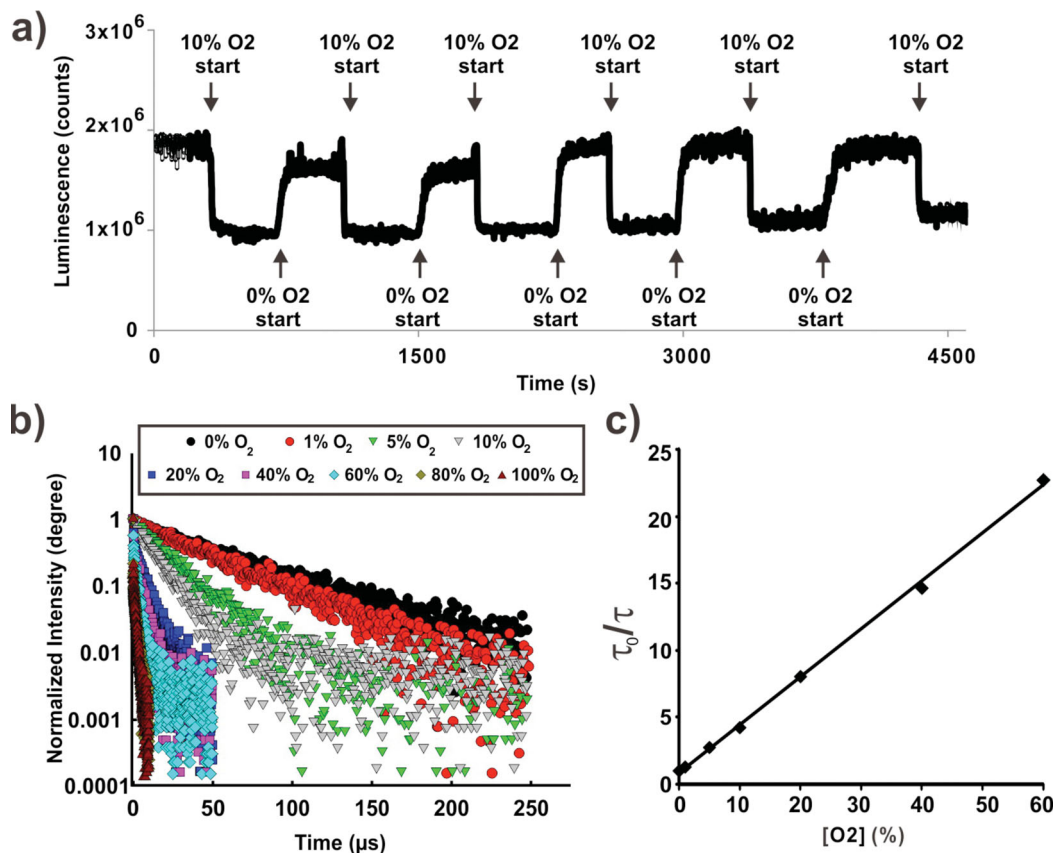
Figure 3. Oxygen-responsive phosphorescence of the Pd-porphyrin hydrogel. a) Reversible steady-state phosphorescence response to oxygen in indicated conditions at 37 °C. b) Characterization of hydrogel phosphorescence lifetime response. c) Stern-Volmer lifetime analysis of hydrogel phosphorescence as a function of oxygen concentration.

polymerization (3×10^{-3}, 4×10^{-3}, and 5×10^{-3} M Pd-mTCPP), the resulting gels displayed markedly different water swelling ratios ranging from ≈4500% for the 3×10^{-3} M concentration to ≈2000% for the 5×10^{-3} M hydrogel. Scanning electron micrographs revealed a hydrogel with a relatively smooth macroscale surface in accordance to the optically reflective hydrogel shown in Figure 1c. At higher magnifications, distinct submicron-sized features were apparent, supporting the existence of a disordered but highly interconnected porphyrin-PEG environment (Figure 2e).

Pd-mTCPP hydrogels featured a typical porphyrin absorption with a Soret band at 416 nm and a lesser Q-band at 523 nm and produced long wavelength phosphorescence around 705 nm. Due to spatial constraint in the matrix, strong luminescence quenching was avoided, which can occur at due to porphyrin–porphyrin interaction at high densities.[37] The hydrogel responses to varying oxygen levels was measured by adsorbing the gel to the side of a water-filled cuvette with bubbling gas and probing the phosphorescence response either in a fluorometer or with a bifurcated optical fiber for lifetime measurements. As shown in **Figure 3**a, by changing the environment of the hydrogel from pure nitrogen to 10% oxygen, a reversible change in phosphorescence was observed. When oxygen was introduced, the phosphorescence of the hydrogel decreased in approximately 15 s. When an oxygen-free environment

was reintroduced, the hydrogel responded with an increase in phosphorescence over a 30 s period. These response times in the tens of seconds and with the low oxygen conditions taking a longer time for equilibration are in line with previously phosphorescence oxygen sensors.[12,13,38,39] Phosphorescent lifetimes were obtained over a wide range of oxygen concentrations using an analog lifetime detection system as previously reported.[40] Phosphorescence lifetimes ranged from 55 μs in oxygen-free conditions to 2.4 μs in 60% oxygen (Figure 3b). The Stern-Volmer lifetime quenching constant was determined using

$$\frac{\tau_0}{\tau} = 1 + K_{SV} \cdot [O_2] \qquad (1)$$

Where τ_0 is the oxygen-free phosphorescence lifetime, τ is the phosphorescence lifetime in varying oxygen concentrations, K_{SV} is the Stern-Volmer curve constant and $[O_2]$ is oxygen concentration. Following unit conversion, a K_{SV} value of 38×10^5 Pa^{-1} was observed, which is similar to previously reported oxygen quenching constants of Pd- and Pt-porphyrins.[41] In this range, which extends well beyond physiological levels of oxygen, the lifetime quenching relationship was linear (with an R^2 value of 0.999) in accordance with the Stern-Volmer quenching expected for collisional quenching of the porphyrins by freely diffused molecular oxygen (Figure 3c).

FULL PAPER
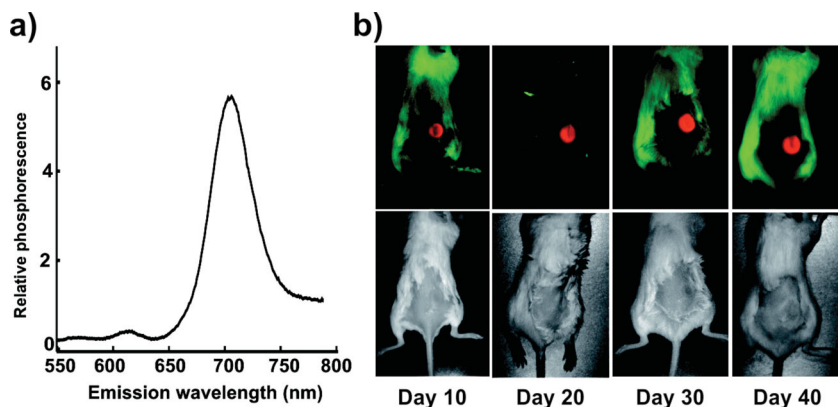
Figure 4. Suitability of the Pd-porphyrin hydrogel for in vivo implantation and transdermal imaging. a) Luminescence emission spectrum in the near infrared of the Pd-porphyrin hydrogel in 20% oxygen. b) Hydrogel was implanted subcutaneously in a BALB/c mouse and imaged every 10 d. Luminescence images are shown in the top row and corresponding white light images are shown in the bottom row. No obvious degradation, photobleaching, or toxicity was observed. Images were acquired on a Maestro imager.

2.2. In Vivo Implantation of Pd-mTCPP Hydrogels

As shown in **Figure 4**a, the hydrogel phosphorescence peak appeared around 705 nm, a wavelength that is in the near-infrared window well-suited for in vivo biological imaging applications.[42] Due to the high porphyrin density that is spatially constrained to prevent self-quenching,[36] we hypothesized that measurement of the Pd-porphyrin hydrogel phosphorescence would be possible in vivo. The hydrogel was implanted with a minor surgical procedure that involved making an incision on the back of BALB/c mice, inserting the hydrogel and closing the incision with sutures. In the future, an injectable hydrogel formulation, either through size modification of the existing hydrogel into microparticles or chemical modification of the material would be beneficial to avoid risks and inconvenience associated with minor surgery. The hydrogel was readily detected through the skin on the back of the mouse. Hydrogel luminescence could clearly be detected over the autofluorescence of background using steady-state luminescence imaging with a short 200 ms camera exposure. Figure 4b shows the implanted hydrogel luminescence 10 d after implantation, after the sutures had been removed. The hydrogel maintained its shape and brightness over a 40-d period without significant degradation or photobleaching. The mouse remained healthy and did not display any outward signs of toxicity. To our knowledge, this is longest in vivo demonstration of a stable, implantable oxygen-sensitive phosphorescent biomaterial. Other oxygen-sensing materials might be rapidly be cleared, degraded, or drained by the body, or alternatively at the high concentrations required for transdermal detection might be self-quenched.

Direct measurement of absolute hydrogel phosphorescence intensity in itself does not provide a reliable measure oxygen levels. Phosphorescence lifetime analysis as shown in Figure 3 provides a more robust measure but setup of such a transdermal phosphorescence lifetime imaging system poses significant technical challenges. Therefore, to obtain a simple measure of oxygen levels, ratiometric approaches may be used.[43] We developed a ratiometric approach that compared total Pd-hydrogel luminescence to the luminescence of a non-oxygen-responsive fluorescent companion hydrogel. Since free base porphyrins are orders of magnitude brighter in comparison to Pd-porphyrins (in normal atmospheric conditions), to prevent detector saturation of the free base porphyrin hydrogel, the total luminescence of the free base porphyrins was attenuated by incorporation of non-luminescent copper tetracarboxy porphyrins (Cu-mTCPP) into the polymer. A series of hydrogels was synthesized with increasing amounts of Cu-mTCPP into a free base porphyrin background (**Figure 5**a). This approach provided a highly tunable method to generate hydrogels that could have their total NIR luminescence readily attenuated while maintaining the polymer structure. Three of these non-oxygen-responsive fluorescent hydrogels (containing 5, 10, and 15% free base-mTCPP with the remaining portion being composed of non-luminescent copper porphyrins) were examined along with the Pd-porphyrin-hydrogel in atmospheres composed of 0%, 10%, or 20% oxygen in nitrogen gas (Figure 5b). As expected, the steady-state luminescence of the free base-copper hydrogels did not vary, whereas the Pd-porphyrin hydrogel luminescence increased greatly as oxygen levels decreased while the maximum phosphorescence emission wavelength remained constant (**Figure 6**b). The Pd-mTCPP and 15% free base-mTCPP hydrogels were co-implanted on the back of BALB/c mice, in the subcutaneous space between the skin and the muscle. After the two hydrogels were placed subcutaneously in a small incision, the skin was sutured closed and was allowed to heal for one week. To demonstrate proof of principle for the new paradigm of dual-hydrogel transdermal ratiometric imaging, we examined a basic scenario where subcutaneous oxygen levels changed. Following anesthization of the mice, they were imaged immediately. They
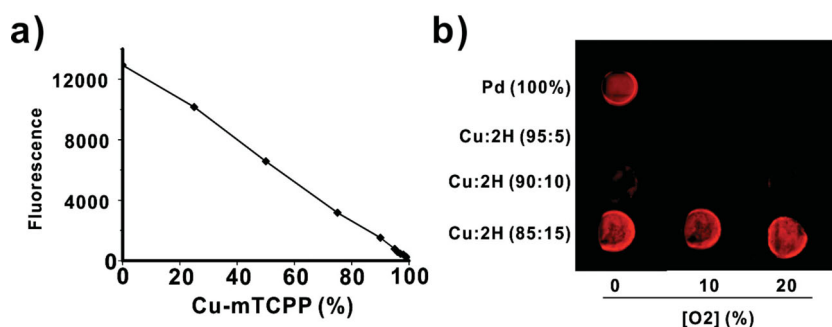
Figure 5. A copper-doped, non-oxygen-responsive companion hydrogel for ratiometric imaging. a) Free base mTCPP could be titrated with non-luminescent Cu-mTCPP to tune overall hydrogel luminescence. b) Luminescence imaging of Pd-mTCPP and freebase-Cu-mTCPP hydrogels in varying oxygen conditions.

a)

b)
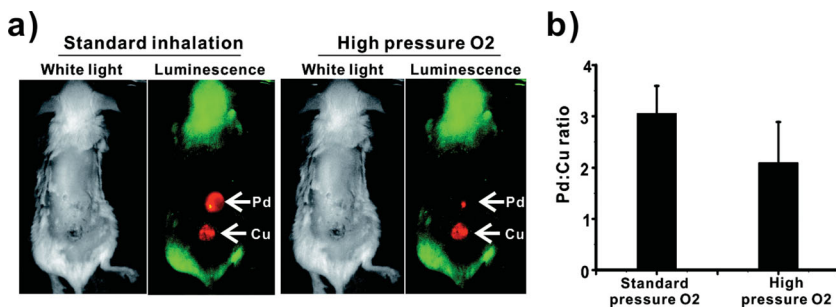
Figure 6. In vivo detection of subcutaneous oxygenation. a) Transdermal luminescence imaging of dual-implanted Pd-mTCPP and 15% free base-Cu-mTCPP hydrogels. Left images were taken following anesthetization and right ones taken following high-pressure oxygen administration. b) Ratiometric changes in Pd and 2H/Cu luminescence over time following mouse exposure to high-pressure inhaled oxygen (error bars show mean ± std. dev. for $n = 3$ separately implanted and treated mice).

were then secured into the nose cone and administered high pressure pure oxygen (3 L min^{-1}) for 45 min. This technique was chosen as it has been demonstrated to increase subcutaneous levels of oxygen in rodents.[44] As shown in Figure 6a, following high-pressure oxygen, the the Pd-mTCPP hydrogel became noticeably dimmer whereas the 2H/Cu hydrogel luminescence remained constant. Figure 6b shows that the ratio of the total luminescence of the two hydrogels decreased reproducibly in the subcutaneous following high-pressure oxygen exposure. To deal with possible optical interference the light by tissues, future studies should be performed to accurately and quantitatively calibrate the obtained in vivo luminescence ratios with direct measurement of subcutaneous oxygen using electrode measurements.

3. Conclusion

We successfully used Pd-porphyrins as PEG cross-linkers to generate a novel hydrogel with oxygen-responsive optical properties. The polymerization reaction was fast and effective and resulted in an extreme density porphyrin hydrogel ($\approx 5 \times 10^{-3}$ M) with a unique 3D network that prevented porphyrin aggregation and associated concentration-dependent quenching. Using an intensity matched non-oxygen-sensitive 2H/Cu porphyrin hydrogel, ratiometric imaging was demonstrated in vivo with a companion hydrogel system. Future work will aim to create an injectable hydrogel system to avoid the need for surgical implantation and to develop a hydrogel with an internal ratiometric standard so that a single hydrogel can be implanted instead of two. The advantage of spectrally resolved, internal ratiometric fluorescence callibration has been demonstrated for oxygen sensors.[36,37] The approach of using porphyrins as covalent conjugation sites for dendrimers has recently been demonstrated,[45] opening the possibility of creating analagous ultra-bright nanoscale porphyrin oxygen sensors.

4. Experimental Section

Synthesis and Characterization of Pd-mTCPP Hydrogel: Chemicals were obtained from Sigma unless otherwise noted. The main components of

the hydrogel were Pd-meso-tetra(4-carboxyphenyl) porphyrin (Cat# PdT790, Frontier Scientific) and diamine-functionalized PEG 6K (Cat# 11 6000–2, Rapp Polymere). Unless otherwise stated, this PEG 6K was used. Pd-mTCPP, PEG 6K, and the acid activator HBTU (O-(Benzotriazol-1-yl)-N,N,N',N'-tetramethyluronium hexafluorophosphate) were dissolved in DMF (N,N-Dimethylformamide) and mixed together with the molar ratio of 1:2:4, at concentrations of 5×10^{-3} M, 10×10^{-3} M, and 60×10^{-3} M, respectively. After adding 40 µL this solution to a polypropylene 96-well plate, 2 µL of 10% DIPEA (N,N-Diisopropylethylamine) in DMF was added to initiate the reaction. The reaction completed within 20 s but was left untouched for at least another 15 min. Excess DMF was then added to first stop the solid polymerization reaction and to wash out unincorporated porphyrins and other materials for 8 h. The DMF was collected and the absorbance was compared to the original solution to obtain polymerization efficiency. This same basic procedure was used to test the various parameters of hydrogel formation. The influence of PEG size was assessed with PEG 2K and PEG 3K (Cat# 11 2000–2 and 11 3000–2, Rapp Polymer). Following removal of DMF, the hydrogel was placed in water to remove excess DMF overnight and remained stored in water. The hydrogel was freeze-dried for scanning electron micrographs (SEM) and water swelling studies. The Pd-mTCPP hydrogel was frozen rapidly in a dry ice/acetone bath and then transferred to a freeze dryer overnight (Freezone, Labconco) to fully remove all water. Swelling efficiency was calculated as the weight of the water swollen gel compared to the weight of the freeze-dried gel. SEM was performed using the freeze-dried polymer on a stage in a vacuum(Auriga dual beam system, Zeiss).

Optical Properties of the Pd-mTCPP Hydrogel: For generating a non-oxygen-responsive companion hydrogel, free base mTCPP and Cu-mTCPP (Cat# T790 and C974, Frontier Scientific) were combined with 0, 20%, 50%, 75%, 90%, 95%, 96%, 97%, 98%, 99%, and 100% copper porphyrin. For each well in a 96-well plate, the volume of the mixed solution and HBTU were both 13.3 µL and 2 µL of 10% DIPEA in DMF was added. 5 min later, 13.4 µL PEG-6K solution was added into into each well and 15 min later DMF was used to wash out unincorporated reactants. A fluorescence plate reader was used to measure the fluorescence of the samples using 415 nm excitation and 680 nm emission with 5.0 nm slit widths (Safire plate reader, TECAN). Oxygen measurements were performed in a mixed gas controlled flow cell that achieved desired levels of oxygenation from two externally tanks (nitrogen and oxygen). Steady-state measurements were performed at 40 °C. Excitation wavelength light was provided by a pulsed dye laser source set a 30° to the plane of the glass. The laser is pulsed by signal generator and connected to an amplified photodetector (Thorlab PDA-100A) through a lock-in amplifier. Data acquisition was performed in real time using a LabView 8.2 interface. Gas was delivered to the hydrogel by channels within a flow cell with the hydrogel adsorbed to the wall of the cuvette. Luminescence collection was completed by photodiode with a 700-nm bandpass filter. Luminescence photographs were taken in a fluorescence imaging system (Maestro, CRI) after hydrogels had been placed in glass cuvettes containing the indicated oxygen concentrations in a nitrogen background and were sealed with parafilm. All time-resolved intensity decay traces were acquired using an oscilloscope-based time-resolved instrument. The excitation source is a VSL-337 pulsed N2 (g) laser (337 nm, $<P> = 2.0$ mW, $P_{max} = 40$ kW); detection is achieved by a fast wired photomultiplier tube (Hamamatsu, model R928) with the output directed to an oscilloscope (Tektronix, model TDS 350).

In Vivo Studies: Animal experiments were conducted in compliance with University at Buffalo Institutional Animal Care and Use Committee policy. Mice were anesthetized with 2% (v/v) isoflurane in 100% oxygen carrier gas. Under deep anesthesia, a small incision was made in skin on the back of the mouse and a Pd-mTCPP and a 15% mTCPP/85%

Cu-mtCPP hydrogel were inserted. Sutures (Reli Black Nylon-monofilament Sutures from MYCO Medical Inc., MYCO Catalog number is N931) were used to close the wound. After surgery, luminescence transdermal photos of the hydrogels were taken in the Maestro imager under isoflurane anesthesia as indicated. For high-pressure inhaled oxygen, turning the button on the anesthesia machine to change the 100% oxygen flow rate was set to 3 L min^{-1}, with the concentration of isoflurane was still 2% (v/v). Mice were subjected the gas for 45 min before imaging.

Supporting Information

Supporting Information is available from the Wiley Online Library or from the author.

Acknowledgements

[1] K. Zhang, L. Zhu, M. Fan, *Front Mol. Neurosci.* **2011**, *4*, 1.
[2] J. F. Schmedtje Jr., Y.-S. Ji, *Trends Cardiovasc. Med.* **1998**, *8*, 24.
[3] M. López-Lázaro, *Anticancer Agents Med. Chem.* **2009**, *9*, 517.
[4] S. Schreml, R. m. Szeimies, L. Prantl, S. Karrer, M. Landthaler, P. Babilas, *Br. J. Dermatol.* **2010**, *163*, 257.
[5] R. Springett, H. M. Swartz, *Antioxidants Redox Signal.* **2007**, *9*, 1295.
[6] F. B. Bolger, S. B. McHugh, R. Bennett, J. Li, K. Ishiwari, J. Francois, M. W. Conway, G. Gilmour, D. M. Bannerman, M. Fillenz, M. Tricklebank, J. P. Lowry, *J. Neurosci. Methods* **2011**, *195*, 135.
[7] Y. Zhang, J. F. Lovell, *Theranostics* **2012**, *2*, 905.
[8] E. Holder, D. Oelkrug, H.-J. Egelhaaf, H. A. Mayer, E. Lindner, *J. Fluoresc.* **2002**, *12*, 383.
[9] C.-S. Chu, *J. Lumin.* **2013**, *135*, 5.
[10] R. P. Briñas, T. Troxler, R. M. Hochstrasser, S. A. Vinogradov, *J. Am. Chem. Soc.* **2005**, *127*, 11851.
[11] M. Obata, Y. Tanaka, N. Araki, S. Hirohara, S. Yano, K. Mitsuo, K. Asai, M. Harada, T. Kakuchi, C. Ohtsuki, *J. Polym. Sci., Part Polym. Chem.* **2005**, *43*, 2997.
[12] T.-S. Yeh, C.-S. Chu, Y.-L. Lo, *Sens. Actuators B Chem.* **2006**, *119*, 701.
[13] A. N. Watkins, B. R. Wenner, J. D. Jordan, W. Xu, J. N. Demas, F. V. Bright, *Appl. Spectrosc.* **1998**, *52*, 750.
[14] C.-S. Chu, Y.-L. Lo, *Sens. Actuators B Chem.* **2008**, *134*, 711.
[15] D. B. Papkovsky, G. V. Ponomarev, W. Trettnak, P. O'Leary, *Anal. Chem.* **1995**, *67*, 4112.
[16] Y. Tian, B. R. Shumway, D. R. Meldrum, *Chem. Mater.* **2010**, *22*, 2069.
[17] Y. Tian, B. R. Shumway, W. Gao, C. Youngbull, M. R. Holl, R. H. Johnson, D. R. Meldrum, *Sens. Actuators B Chem.* **2010**, *150*, 579.
[18] H. Lu, Y. Jin, Y. Tian, W. Zhang, M. R. Holl, D. R. Meldrum, *J. Mater. Chem.* **2011**, *21*, 19293.
[19] A. Y. Lebedev, A. V. Cheprakov, S. Sakadžić, D. A. Boas, D. F. Wilson, S. A. Vinogradov, *ACS Appl. Mater. Interfaces* **2009**, *1*, 1292.
[20] D. F. Wilson, G. J. Cerniglia, *Cancer Res.* **1992**, *52*, 3988.
[21] S. Sakadžić, E. Roussakis, M. A. Yaseen, E. T. Mandeville, V. J. Srinivasan, K. Arai, S. Ruvinskaya, A. Devor, E. H. Lo, S. A. Vinogradov, D. A. Boas, *Nat. Methods* **2010**, *7*, 755.
[22] I. Vanzetta, A. Grinvald, *Science* **1999**, *286*, 1555.
[23] L. S. Ziemer, W. M. F. Lee, S. A. Vinogradov, C. Sehgal, D. F. Wilson, *J. Appl. Physiol.* **2005**, *98*, 1503.
[24] R. D. Shonat, D. F. Wilson, C. E. Riva, M. Pawlowski, *Appl. Opt.* **1992**, *31*, 3711.
[25] I. Dunphy, S. A. Vinogradov, D. F. Wilson, *Anal. Biochem.* **2002**, *310*, 191.
[26] R. J. Meier, S. Schreml, X. Wang, M. Landthaler, P. Babilas, O. S. Wolfbeis, *Angew. Chem. Int. Ed.* **2011**, *50*, 10893.
[27] H. Xiang, L. Zhou, Y. Feng, J. Cheng, D. Wu, X. Zhou, *Inorg. Chem.* **2012**, *51*, 5208.
[28] Z. Li, Z. Wei, F. Xu, Y. H. Li, T. J. Lu, Y. M. Chen, G. J. Zhou, *Macromol. Rapid Commun.* **2012**, *33*, 1191.
[29] Z. Xie, L. Ma, K. E. deKrafft, A. Jin, W. Lin, *J. Am. Chem. Soc.* **2010**, *132*, 922.
[30] A. S. Hoffman, *Adv. Drug Delivery Rev.* **2012**, *64*, 18.
[31] J. L. Drury, D. J. Mooney, *Biomaterials* **2003**, *24*, 4337.
[32] T. R. Hoare, D. S. Kohane, *Polymer* **2008**, *49*, 1993.
[33] D. Seliktar, *Science* **2012**, *336*, 1124.
[34] Y. Zhang, B. Zhang, Y. Kuang, Y. Gao, J. Shi, X. X. Zhang, B. Xu, *J. Am. Chem. Soc.* **2013**, *135*, 5008.
[35] I. Klimant, O. S. Wolfbeis, *Anal. Chem.* **1995**, *67*, 3160.
[36] J. F. Lovell, J. Roxin, K. K. Ng, Q. Qi, J. D. McMullen, R. S. DaCosta, G. Zheng, *Biomacromolecules* **2011**, *12*, 3115.
[37] J. F. Lovell, C. S. Jin, E. Huynh, H. Jin, C. Kim, J. L. Rubinstein, W. C. W. Chan, W. Cao, L. V. Wang, G. Zheng, *Nat. Mater.* **2011**, *10*, 324.
[38] S. M. Borisov, C. Krause, S. Arain, O. S. Wolfbeis, *Adv. Mater.* **2006**, *18*, 1511.
[39] Y. Amao, T. Miyashita, I. Okura, *J. Fluorine Chem.* **2001**, *107*, 101.
[40] Y. Tang, E. C. Tehan, Z. Tao, F. V. Bright, *Anal. Chem.* **2003**, *75*, 2407.
[41] S. M. Borisov, V. V. Vasil'ev, *J. Anal. Chem.* **2004**, *59*, 155.
[42] Y. Amao, I. Okura, *J. Porphyrins Phthalocyanines* **2009**, *13*, 1111.
[43] C. Wu, B. Bull, K. Christensen, J. McNeill, *Angew. Chem. Int. Ed.* **2009**, *48*, 2741.
[44] M. W. Dewhirst, E. T. Ong, G. L. Rosner, S. W. Rehmus, S. Shan, R. D. Braun, D. M. Brizel, T. W. Secomb, *Br. J. Cancer. Suppl.* **1996**, *27*, S241.
[45] A.-L. Wirotius, E. Ibarboure, L. Scarpantonio, M. Schappacher, N. D. McClenaghan, A. Deffieux, *Polym. Chem.* **2013**, *4*, 1903.